

Investigating the interactions of a novel anticancer DLC and its precursor compound with serum albumin

Supporting Information

Content

Fig. SI 1 ^1H NMR of PVI and F16 in DMSO- d_6 .

Fig. SI 2 Mass spectrum of PVI and F16.

Fig. SI 3 Arrhenius plots of F16-HSA system.

Fig. SI 4 Effect of PVI and F16 on the synchronous fluorescence spectrum of HSA.

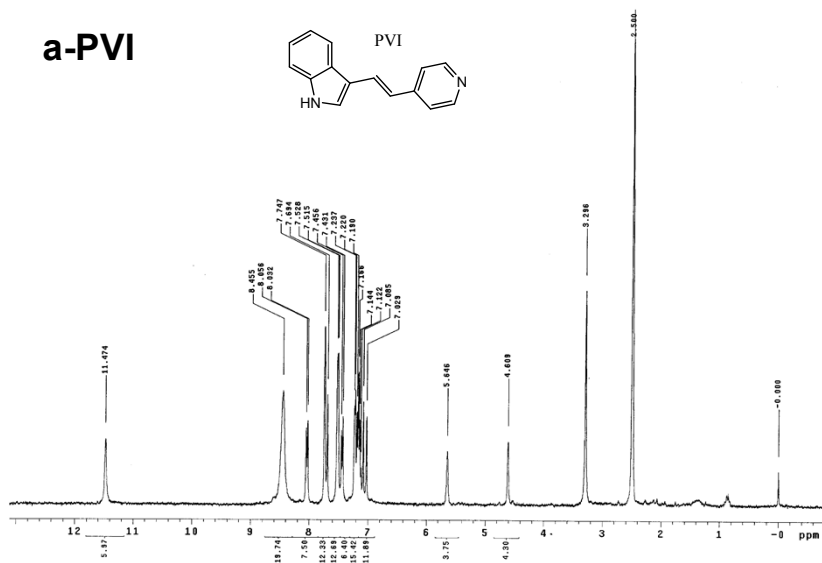
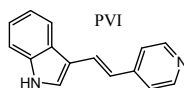
Fig. SI 5 Contour map of three-dimensional fluorescence spectra.

Fig. SI 6 Detailed illustration of the interactions between PVI and HSA.

Fig. SI 7 Detailed illustration of the interactions between F16 and HSA.

Ba1012.20-3

a-PVI



XiangC10.27-1

Archive directory: /export/home/xu/vmr/sys/data
Sample directory:
File: PROTON

Pulse Sequence: s2pu1

b-F16

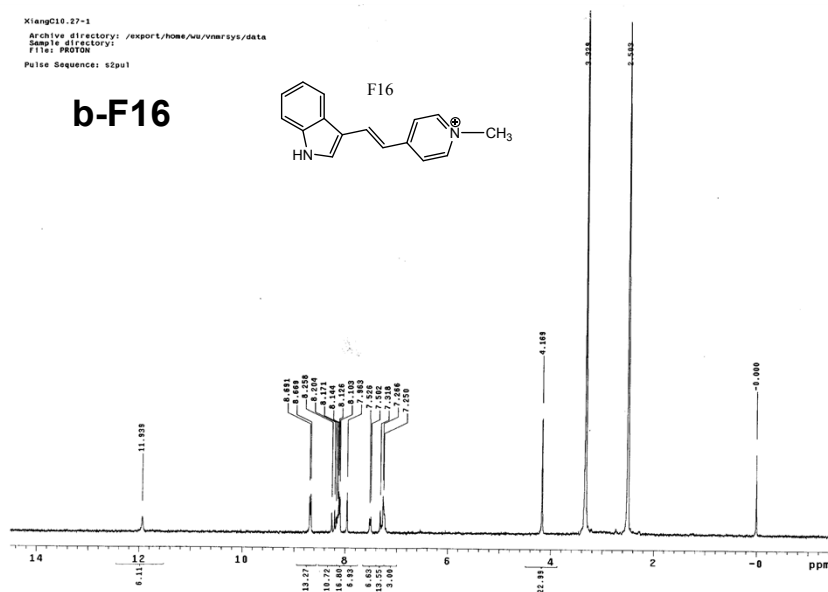
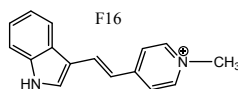


Fig. SI 1 ^1H NMR of (a) PVI and (b) F16 in DMSO-d_6 . PVI: δ 7.029-7.122(m, 2H), 7.144-7.237(m, 2H), 7.456(d, $J = 7.5$ Hz, 1H), 7.528 (d, $J = 4.5$ Hz, 2H), 7.747(d, $J = 15$ Hz, 2H), 8.056(d, $J = 7.2$ Hz, 2H), 11.474(s, 1H). F16: δ 4.169(s, 3H), 7.250-7.266(m, 2H), 7.318(s, 1H), 7.526(d, $J = 7.5$ Hz, 1H), 7.963(s, 1H), 8.103-8.126(m, 2H), 8.144-8.258(m, 2H), 8.669-8.691(d, $J = 2.4$ Hz, 2H), 11.939(s, 1H).

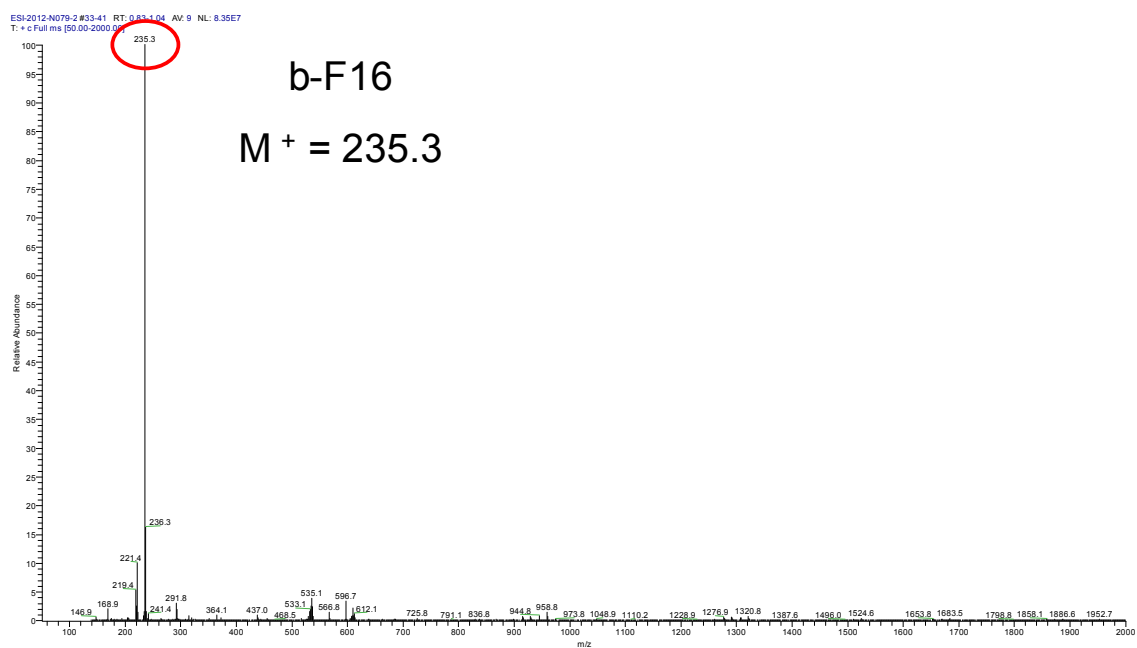
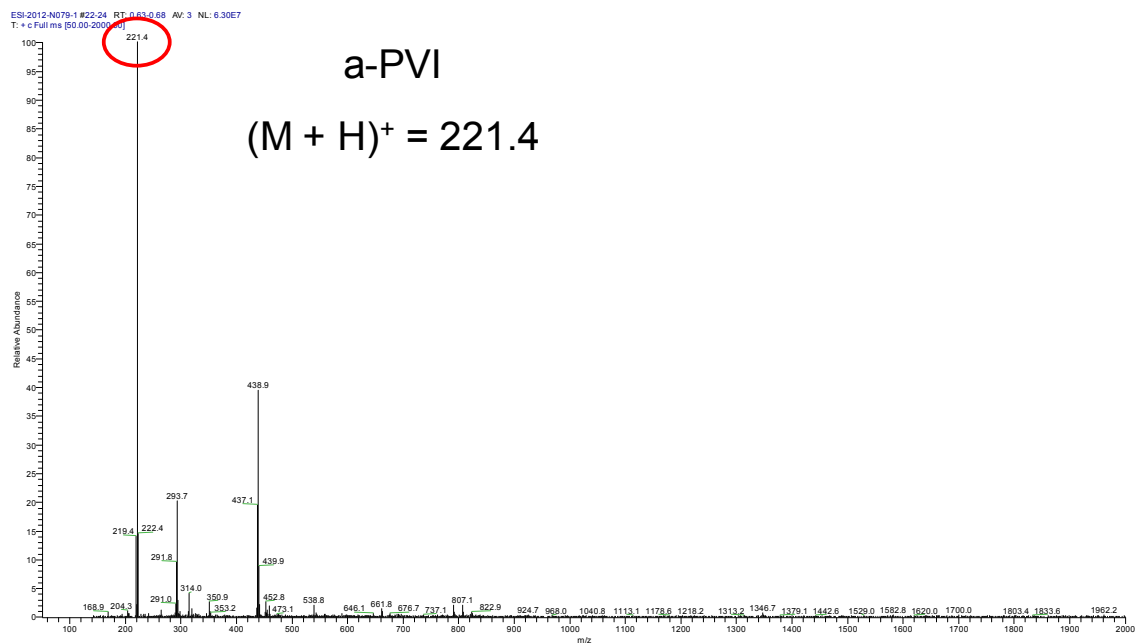


Fig. SI 2 Mass spectrum of (a) PVI and (b) F16.

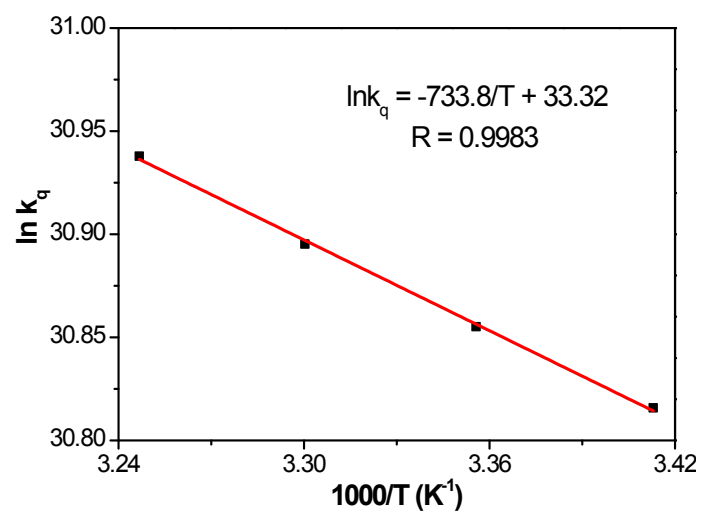


Fig. SI 3 Arrhenius plots of F16-HSA system.

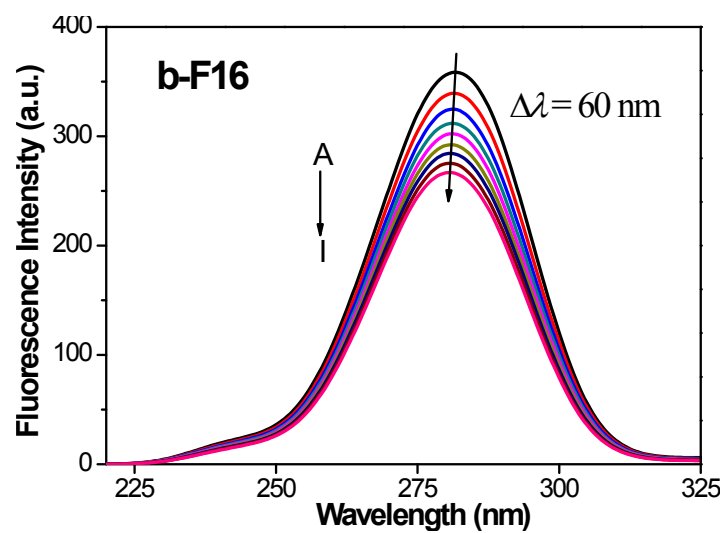
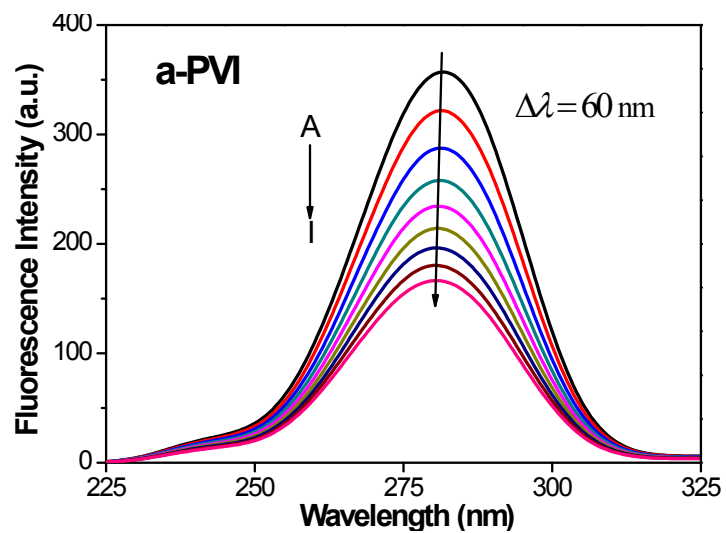


Fig. SI 4 Effect of (a) PVI and (b) F16 on the synchronous fluorescence spectrum of HSA. $\Delta\lambda = 60$ nm; $c(\text{HSA}) = 1.0 \times 10^{-5}$ mol L⁻¹; $c(\text{PVI or F16})/(10^{-6}$ mol L⁻¹) (A-I): 0; 2; 4; 6; 8; 10; 12; 14; 16.

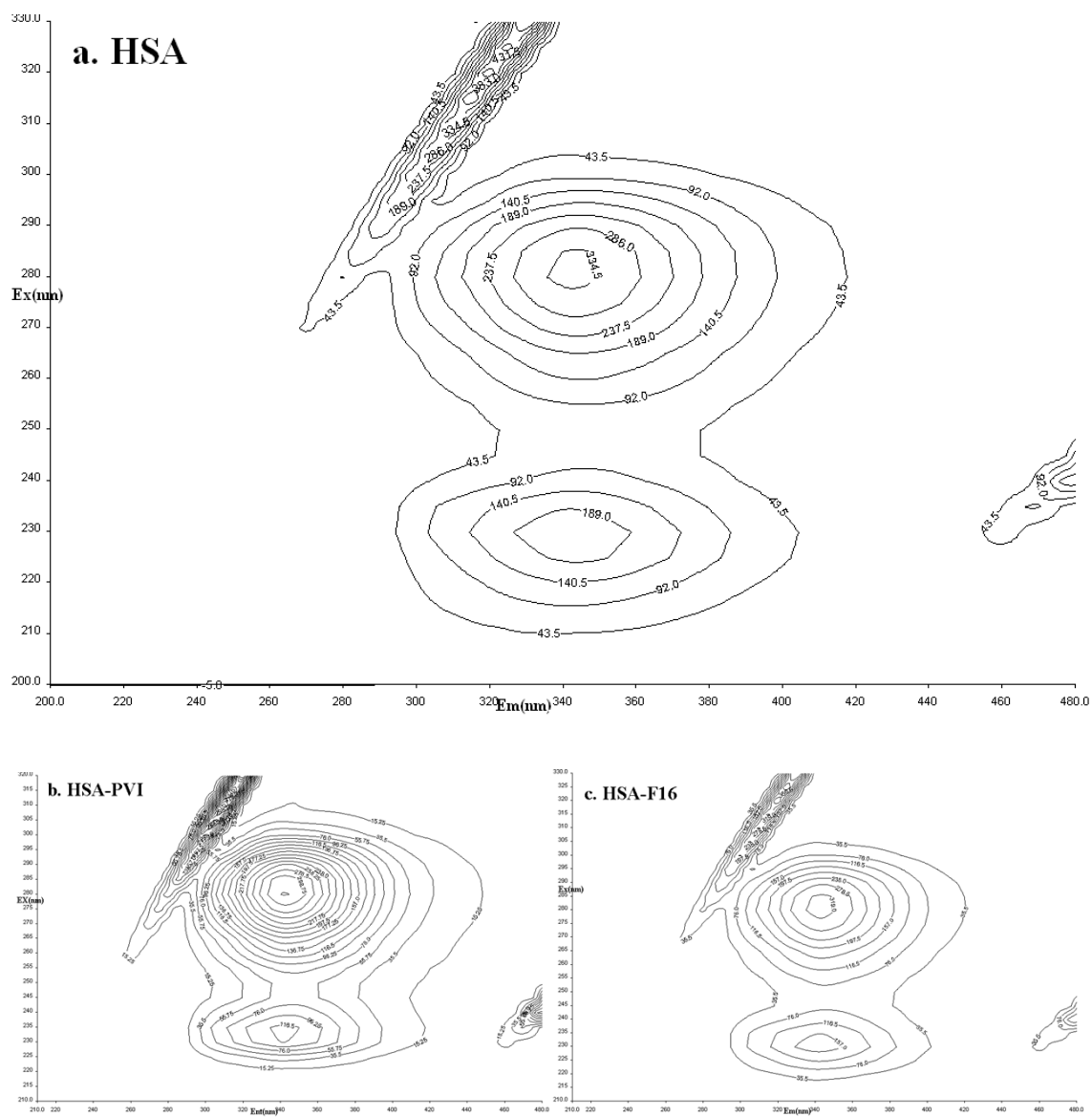


Fig. SI 5 Contour map of three-dimensional fluorescence spectra of (a) HSA only, (b) HSA-PVI system and (c) HSA-F16 system. $c(\text{HSA}) = c(\text{PVI or F16}) = 2 \times 10^{-6} \text{ mol L}^{-1}$.

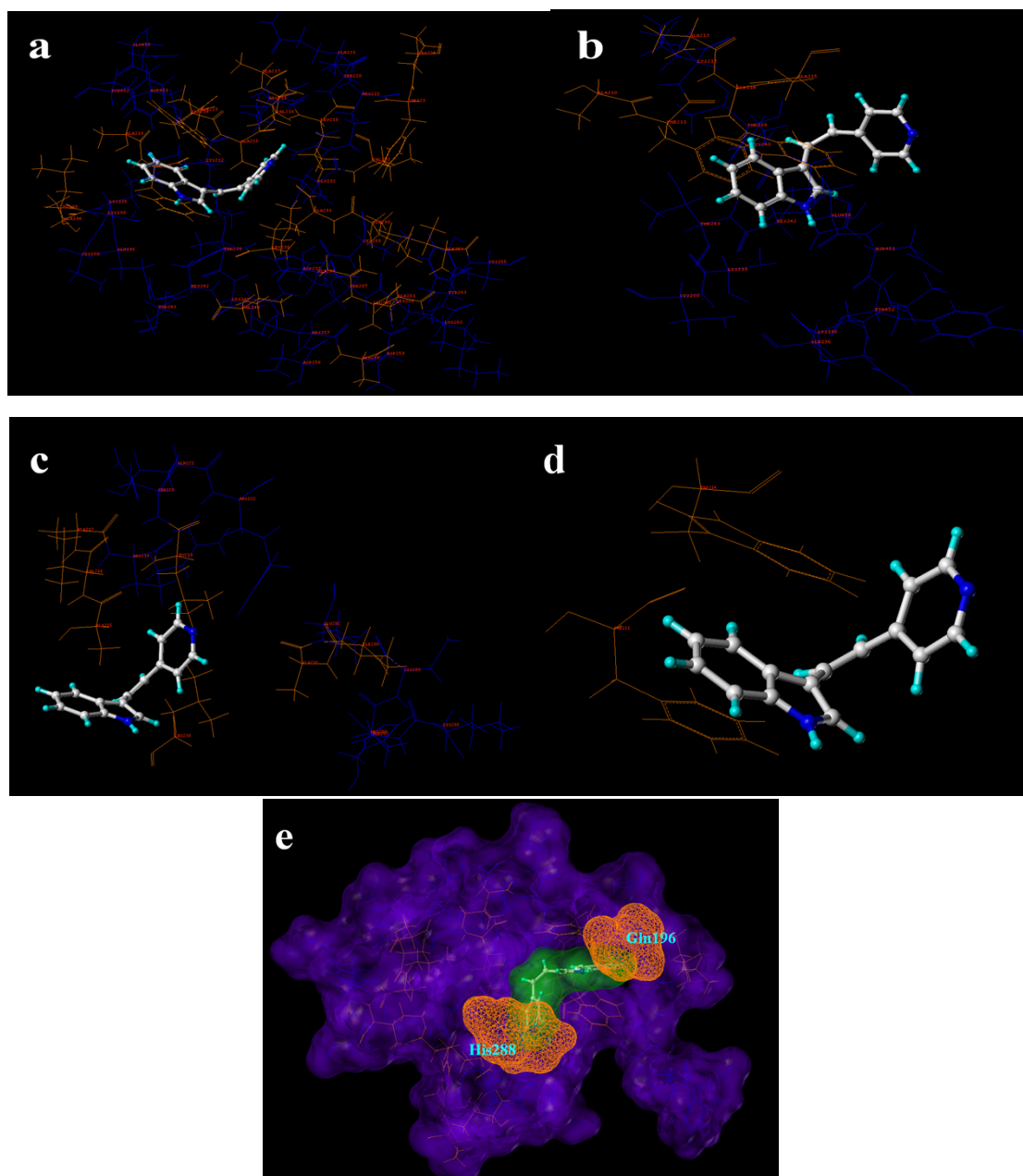


Fig. SI 6 Detailed illustration of the interaction between PVI and HSA. (a) The detailed binding site in HSA and the conformation of PVI. Hydrophobic amino acid residues are shown in orange, while hydrophilic amino acid residues are shown in blue. (b) The indole group is enclosed by a hydrophobic loop comprised with Ala210, Phe211, Ala213, Trp214 and Ala215. (c) The pyridine group inserts into a hydrophobic loop made up of Ala215, Val216, Leu219, Leu238 and Ala291. (d) The spatial relation of the

indole group and Trp214. (e) The surface model of PVI in the binding site. The surface of the HSA binding site is shown in purple, while Gln196 and His288 are shown in orange. The surface of PVI is shown in green.

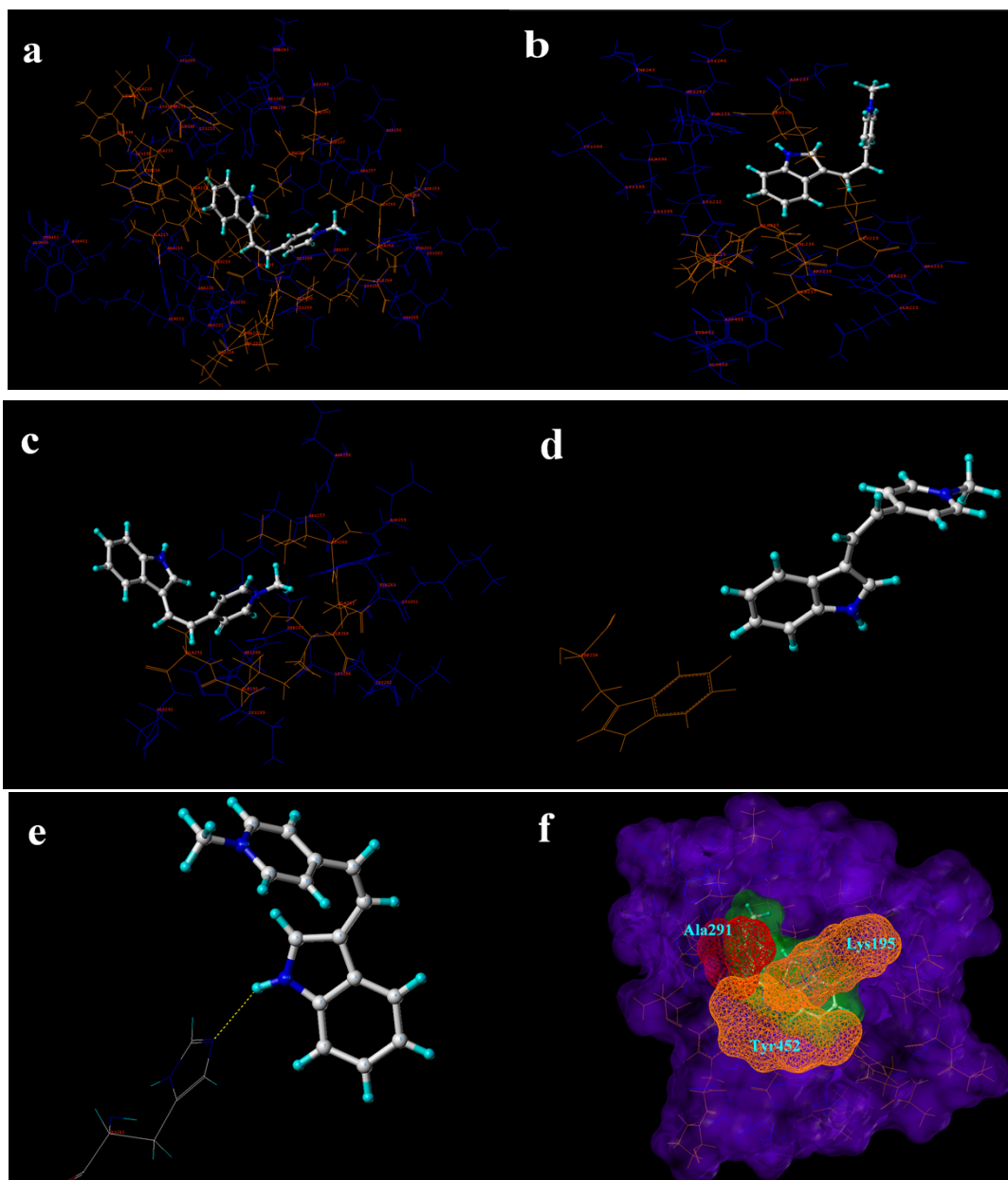


Fig. SI 7 Detailed illustration of the interaction between F16 and HSA. (a) The detailed binding site in HSA and the conformation of F16. Hydrophobic amino acid residues are shown in orange, while hydrophilic amino acid residues are shown in blue. (b) The indole group is surrounded by a hydrophobic loop composed by Ala215, Ala217, Leu219, Leu238 and Trp244. (c) The pyridine group of F16 inserts into a hydrophobic loop consisting of Leu260, Ala261, Ile264, Ile290 and Ala291, while the methyl group inserts into the gap between Leu260 and Ile264. (d) The spatial relation of the indole group and Trp214. (e) Detailed illustration of the hydrogen bond formation, NE2 in His242 forms a hydrogen bond with H10 in F16. (f) The surface model of F16 in the binding site. The surface of the HSA binding site is shown in purple and the surface of F16 is shown in green. The outside obstacles of HSA-F16 system (Lys195 and Tyr452) are shown in orange and the inside one (Ala291) is shown in red.